A State Transition Diagram for Simultaneous Collisions with Application in Billiard Shooting

Yan-Bin Jia[1], Matthew T. Mason[2], and Michael A. Erdmann[2]

[1] Department of Computer Science, Iowa State University, `jia@cs.iastate.edu`
[2] School of Computer Science, Carnegie Mellon University,
   `{mason+,me}@cs.cmu.edu`

Abstract. This paper models a multibody collision in the impulse space as a state transition diagram, where each state represents a phase during which impacts are "active" at only a subset of the contact points. A state transition happens whenever an active impact finishes restitution, or an inactive impact gets reactivated, depending on whether the two involved bodies are instantaneously penetrating into each other or not. The elastic energy due to an impact is not only affected by the impulse at the corresponding contact point, but also by other impulses exerted on the two involved bodies during the impact. Consequently, Poisson's impulse-based law of restitution could result in negative energy. A new law governing the loss of elastic energy during restitution is introduced. Convergence of the impulse sequence generated by the state transition diagram is established. The collision outcome depends on the ratios of the contact stiffnesses rather than on their individual values. The collision model is then applied in an analysis of billiard shooting in which the cue stick impacts the cue ball, which in turn impacts the pool table.

1 Introduction

Analysis of frictional impact has been a subject of controversy in order to be consistent with Coulomb's law of friction, Poisson's hypothesis of restitution, and the law of energy conservation. It requires correct detection of contact modes (sliding, sticking, reverse sliding) and impact phases (compression and restitution). When the sliding direction stays constant (with possible reversals), the tangential impulse can be determined from the normal impulse based on Coulomb's law via case-based reasoning. The total impulse stays in the plane and grows along a polyline. Routh [15] developed a graphical method that constructs the trajectory of impulse accumulation based on Poisson's hypothesis. It was applied in the subsequent studies of two-dimensional rigid-body collisions with friction by Han and Gilmore [6] and by Wang and Mason [18] who classified impact and contact modes and offered a solution for each case. Later, Ahmed *et al.* [1] extended Routh's method to impact analysis for multibody mechanical systems with a similar classification.

To an impact in three dimensions, however, Routh's method hardly applies since the impulse builds along a space curve. The sliding direction generally varies during the impact. A differential equation in the normal impulse

can be set up and solved to determine how the sliding direction varies in the course of the impact, as shown by Keller [9]. Closed-form solution does not exist for many three-dimensional impact problems.

This paper deals with simultaneous collisions in three dimensions. No existing impact laws are known to model the physical process well. Previous methods either sequence them into two-body collisions [5] by order of normal approach velocity, or set up linear complementarity conditions at all contacts [16,2]. High-speed photographs of such collisions nonetheless show that multiple objects are simultaneously in contact rather than two at a time [17].

Stewart [17] pointed out that one difficulty with multiple contacts lies in the lack of a continuous impact law. Observations seem to suggest, during simultaneous collisions, the involved objects may have broken and re-established contacts multiple times. We represent the collision process as a sequence of states based on which impacts are instantaneously "active", or equivalently, which contacts are instantaneously effective. During a state, *multiple impacts may be acting upon one body.* A transition from one state to another happens when either an active impact finishes restitution or an inactive impact gets reactivated. A state transition diagram is introduced in Section 2 via the example of a ball falling onto another resting on the table.

The impulses produced by a pair of active impacts accumulate at a relative rate determined by themselves and by the stiffness ratio. The elastic energy stored at one contact point is no longer affected by just the impulse at this point, but also by those at other contact points involving one or both of these two bodies in the duration of this impact, which could span multiple states. Poisson's hypothesis may lead to overgrowth of an impulse during restitution, driving the contact elastic energy negative sometimes. The solution is to introduce a new law of restitution that *oversees the loss of elastic energy not the growth of impulse.*[1] We will also see that the outcome of impact is affected by the ratios of stiffnesses at the contact points. This concept of "relative stiffness" is cited in [17] as missing from the current impact literature.

Section 3 applies the state transition diagram to model billiard shooting with a cue stick. This is a three-dimensional problem with simultaneous impacts between the cue stick and the cue ball, and between the cue ball and the pool table. Analysis of frictional contact modes is required.

In Section 4, we will discuss the extension to simultaneous collisions involving three or more bodies, and introduce an ongoing project to build a robot pool player.

2   System of Two Balls

We start by considering the problem of a rigid ball $\mathcal{B}_1$ with mass m_1 and velocity $v_0 < 0$ striking down onto another rigid ball $\mathcal{B}_2$ with mass m_2 and

---

[1] The roles of the coefficients of restitution and friction were discussed in respect of energy loss [4], and solutions were given to two planar single-impact problems.

resting on a table. The centers of the two balls are vertically aligned, as shown on the left in Fig. 1. The lower ball $\mathcal{B}_2$ in turn impacts the table. Let v_1 and v_2 be the respective velocities (< 0 if downward) of the two balls during the collision, where the gravitational forces are negligible compared to the large impulsive forces. Our goal is to determine the ball velocities at the end.

We attach a virtual spring between $\mathcal{B}_1$ and $\mathcal{B}_2$, and another one between $\mathcal{B}_2$ and the table, as shown on the right in Fig. 1. Let x_1 and x_2 be the changes in the lengths of these springs, which have stiffnesses k_1 and k_2, respectively. The kinematic and dynamic equations are given below:

$$\dot{x}_1 = v_1 - v_2, \tag{1}$$

$$\dot{x}_2 = v_2, \tag{2}$$

$$m_1 \dot{v}_1 = F_1 \quad = \quad -k_1 x_1, \tag{3}$$

$$m_2 \dot{v}_2 = F_2 - F_1 \quad = \quad k_1 x_1 - k_2 x_2, \tag{4}$$
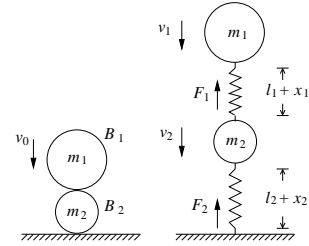
Fig. 1. Two-ball collision.

where F_1 and F_2, both positive, are the contact forces, and the dot '·' denotes differentiation with respect to time. The above are a system of four differential equations in four variables v_i and x_i, $i = 1, 2$.

Since an impact happens in infinitesimal time, it is best analyzed in the impulse space. During the two-ball collision, there are two impulses: $I_1 = \int_{t_0}^{t} F_1 \, dt$ and $I_2 = \int_{t_0}^{t} F_2 \, dt$ with initial values $I_1^{(0)} = I_2^{(0)} = 0$. Integration of (3) and (4) yields the ball velocities in terms of the impulses:

$$v_1 = v_1^{(0)} + \frac{1}{m_1} \Delta I_1, \qquad \text{where } \Delta I_1 = I_1 - I_1^{(0)}, \tag{5}$$

$$v_2 = v_2^{(0)} + \frac{1}{m_2} (\Delta I_2 - \Delta I_1), \qquad \text{where } \Delta I_2 = I_2 - I_2^{(0)}. \tag{6}$$

The two virtual springs store elastic energies $E_1 = \frac{1}{2} k_1 x_1^2$ and $E_2 = \frac{1}{2} k_2 x_2^2$, respectively. To eliminate x_1, from equations (1), (3), (5), (6) we obtain

$$\frac{dx_1}{dI_1} = \frac{\dot{x}_1}{\dot{I}_1} = \frac{v_1^{(0)} - v_2^{(0)} + (\frac{1}{m_1} + \frac{1}{m_2}) \Delta I_1 - \frac{1}{m_2} \Delta I_2}{-k_1 x_1}. \tag{7}$$

Multiply both sides of the above equation with $-k_1 x_1 dI_1$ and then integrate. We obtain the change in the elastic energy E_1 from its initial value $E_1^{(0)}$:

$$\Delta E_1 = \left(v_2^{(0)} - v_1^{(0)} \right) \Delta I_1 - \frac{1}{2} \left(\frac{1}{m_1} + \frac{1}{m_2} \right) \Delta I_1^2 + \frac{1}{m_2} \int_{I_1^{(0)}}^{I_1} \Delta I_2 \, dI_1. \tag{8}$$

Similarly, from equations (2) and (6) we derive the change in E_2 from $E_2^{(0)}$:

$$\Delta E_2 = -v_2^{(0)} \Delta I_2 - \frac{1}{2m_2} \Delta I_2^2 + \frac{1}{m_2} \int_{I_2^{(0)}}^{I_2} \Delta I_1 \, dI_2. \tag{9}$$

A relationship between the two impulses I_1 and I_2 can be now set up:

$$\frac{dI_2}{dI_1} = \frac{\dot{I}_2}{\dot{I}_1} = \frac{k_2 x_2}{k_1 x_1} = \frac{\sqrt{k_2 E_2}}{\sqrt{k_1 E_1}} = \sqrt{\frac{k_2}{k_1}} \cdot \sqrt{\frac{E_2^{(0)} + \Delta E_2}{E_1^{(0)} + \Delta E_1}}. \tag{10}$$

With no closed-form solution to (10) in general, the impact process is simulated via numerical integration with a step size of I_1, say, h. To initialize $\rho = \frac{dI_2}{dI_1}(h)$, we plug into (8)–(10) the values $I_1(h) = h$, $I_2(h) \approx \rho h$, and $\int_0^h \Delta I_2 \, dI_1 = \int_0^{\rho h} \Delta I_1 \, dI_2 \approx \frac{1}{2}\rho h^2$. Solve the resulting quadratic equation in ρ:

$$\frac{dI_2}{dI_1}(h) = \frac{2k_2}{k_1 \cdot (b + \sqrt{b^2 + 4k_2/k_1})}, \quad \text{where } b = -2 \cdot \frac{m_2 v_0}{h} - 1 - \frac{m_2}{m_1} + \frac{k_2}{k_1}. \tag{11}$$

As h tends to zero, b goes to infinity. Hence $\frac{dI_2}{dI_1}(0) = \lim_{h \to 0} \rho = 0$.

2.1 State Transition Diagram

An impact is divided into two stages [12, p. 212]: compression and restitution. In the classical problem of a particle of mass m with downward velocity v_0 striking a horizontal table, the impact ends compression when the velocity becomes zero, which gives the impulse $I = -mv_0$. Poisson's hypothesis states that I will accumulate $-emv_0$ more during restitution to yield the final velocity $-ev_0$, where e is the coefficient of friction. Setting up a virtual spring at the contact point, we can derive the elastic energy $E = -v_0 I - \frac{1}{2m} I^2$. Restitution starts with E assuming the maximum value $\frac{1}{2}mv_0^2$ and ends with loss of energy $\frac{1}{2}mv_0^2 \cdot (1 - e^2)$. Since $0 \leq e \leq 1$, there is always enough elastic energy to provide the impulse accumulation $-emv_0$ during restitution.

Coming back to the two-ball collision problem, the ball-ball and ball-table impacts have coefficients of restitution $e_1, e_2 \in [0, 1]$, respectively. Compressions end when $\dot{x}_1 = 0$ and $\dot{x}_2 = 0$, respectively; or equivalently, by (1), (2), (5), and (6), when

$$v_0 + \left(\frac{1}{m_1} + \frac{1}{m_2}\right) I_1 - \frac{1}{m_2} I_2 = 0 \quad \text{and} \quad I_1 = I_2, \quad \text{respectively.} \tag{12}$$

The two impacts will hardly start restitution at the same time, neither will they end restitution so. When one of them, say, between the two balls, finishes restitution first, the other one (between the ball and the table) will continue. As a result, the two balls may start moving toward each other at some point later, reactivating the first impact.

The above discussion suggests us to partition the collision process into (repeats of) three states: S_1 when both impacts are active, S_2 when only the ball-table impact is active, and S_3 when only the ball-ball impact is active. Fig. 2 shows a state transition diagram. The collision starts with the state S_1.
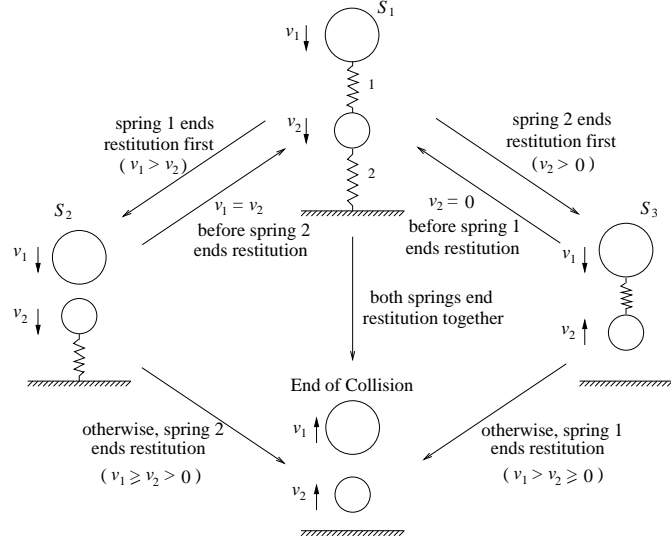
Fig. 2. State transition diagram for the two-ball collision in Fig. 1. During each state, v_1 and v_2 can be either upward or downward, except v_2 is upward in S_3.

A transition from S_1 to S_2 happens when the ball-ball impact finishes restitution before the ball-table impact. So the two balls are "breaking" contact momentarily. Since the impulse I_1 was in restitution just before the transition, $\dot{x}_1 > 0$, which by (1) implies $v_1 > v_2$ when S_2 begins. Because gravity is neglected during the collision, v_1 will not vary during S_2. The state will transition back to S_1 when v_2 increases to become equal to v_1 before restitution ends. If this does not happen, the ball-table impact will finish restitution with $v_1 \geq v_2$, hence the end of collision.

Similarly, a transition from S_1 to S_3 happens when the ball-table impact finishes restitution before the ball-ball impact. The state S_3 will transition to S_1 when $v_2 = 0$, that is, when the lower ball is "re-establishing" contact with the table. Otherwise, the collision will end within the state.

The transition diagram describes the collision as a sequence of states, each being one of S_1, S_2, S_3. Now, I_i, $i = 1, 2$, represent the impulses accumulated since the start of the collision. An impact may start with one state, end compression in another, and finish restitution with a third.

By induction on the number of states, we can generalize (5) and (6):

$$v_1 = v_0 + \frac{1}{m_1} I_1 \quad \text{and} \quad v_2 = \frac{1}{m_2}(I_2 - I_1). \tag{13}$$

It is easy to show that the conditions (12) respectively hold when the two impacts end their compressions in a state.

2.2   An Energy-Based Model

The superscript '(0)' continues to refer to the value of a physical quantity at the start of a state, and the notation 'Δ' its increment so far in the state. The relationship (8) between ΔE_1 and ΔI_1 in the state S_1 depends on the masses and initial velocities of both balls, as well as an integral of ΔI_2 over I_1. If we were to let the impulse I_1 accumulate by a factor of e_1 after restitution under Poisson's hypothesis, there may not be enough elastic energy E_1 left to provide such an increase.[2] To deal with multiple simultaneous impacts, we limit *the amount of energy to be released during restitution relative to the amount accumulated during compression*. Since in the single particle impact case, the loss of energy is $\frac{1}{2}mv_0^2 \cdot (1 - e^2)$, we see that e^2 is the needed ratio.

When compression ends, the elastic energy is at its maximum $E_{\max}$. *Restitution will finish when $E = (1 - e^2)E_{\max}$.* The remaining amount $e^2 E_{\max}$ can be seen as lost at the state transition instead of at the end of compression. In this view, during a state, equations (8) and (9) hold for our convenience, while the total (elastic and dynamic) energy is conserved.

Single-Impact States   The state S_2 starts with $v_2^{(0)} < v_1^{(0)}$ since restitution of the ball-ball impact has just finished. During the state, $v_1 \equiv v_1^{(0)}$ and $\Delta I_1 \equiv 0$. From (6), we conclude that restitution, if not in process, would happen during the state when $\Delta I_2 = -m_2 v_2^{(0)}$ with $E_{2\max} = E_2^{(0)} + \frac{1}{2}m_2 v_2^{(0)\,2}$ by (9). The next state will be S_1 if S_2 starts during compression and $v_1^{(0)} < 0$. Since v_2 increases toward zero by (6), it will reach $v_1^{(0)}$ before compression ends, hence the transition to S_1. Under the new energy-based model, a transition to S_1 will also happen if S_2 starts during restitution with $E_2^{(0)} + \frac{1}{2}m_2 v_2^{(0)\,2} > \frac{1}{2}m_2 v_1^{(0)\,2} + (1 - e_2^2)E_{2\max}$. If neither case of transition happens, the collision will end. The impulse accumulation during S_2 is

$$\Delta I_2 = \begin{cases} m_2(v_1^{(0)} - v_2^{(0)}), & \text{if } S_1 \text{ next}, \\[2ex] m_2\left(\sqrt{v_2^{(0)\,2} + 2\frac{E_2^{(0)} - (1 - e_2^2)E_{2\max}}{m_2}} - v_2^{(0)}\right), & \text{if impact ends}. \end{cases}$$

A similar analysis based on (8) applies to S_3 in determining whether the collision will end or S_1 will follow, and the amount ΔI_1 during S_3.

Double-Impact State   Evolution in the state S_1 is governed by the differential equation (10) with increasing impulses I_1 and I_2. If S_1 is the start of the collision or follows S_3, I_1 is the *primary* impulse (variable), and I_2 is the *secondary* impulse (function of I_1). If S_1 follows S_2, the roles of the two impulses reverse. Similar to (11), we initialize the impulse derivatives $\frac{dI_1}{dI_2}(h)$ or $\frac{dI_2}{dI_1}(h)$ accordingly for numerical integration. Again, $\frac{dI_1}{dI_2}(0) = 0$ and $\frac{dI_2}{dI_1}(0) = 0$, respectively, in these two cases.

---

[2] An example will be given at the end of Section 2.3.

At each step of the numerical integration of (10), we check (12) to see if compression has just ended for either impact, and if so, set the maximum elastic energy $E_{1\max}$ or $E_{2\max}$ accordingly. The state transitions to S_2 when $E_1 = (1 - e_1^2) \cdot E_{1\max}$ during restitution of the ball-ball impact, or to S_3 when $E_2 = (1 - e_2^2) \cdot E_{2\max}$ during restitution of the ball-table impact, whichever occurs earlier.

2.3 The Impulse Curve

In the state S_1, the differential equation (10), along with (8) and (9), has only one occurrence of the stiffness ratio $\frac{k_2}{k_1}$ but none of k_1 or k_2 separately. Meanwhile, the outcome of the states S_2 and S_3 are independent of k_1 or k_2.

Theorem 1. *The outcome of the collision depends on the stiffness ratio k_1/k_2 but not on individual values of k_1 and k_2.*

The next theorem bounds the total elastic energy using the impulses.

Theorem 2. *The following is satisfied during the collision:*

$$0 \le E_1 + E_2 \le -v_0 I_1 - \frac{1}{2m_1} I_1^2 - \frac{1}{2m_2}(I_1 - I_2)^2. \tag{14}$$

Proof. By induction on the number of states while making use of equations (8), (9), and (13). Details are omitted.

In the plane with I_1 and I_2 as the two axes, the *impulse curve* describes the evolution of their values during the collision. Theorem 2 states that this curve is bounded by an ellipse:

$$\frac{1}{2m_1} I_1^2 + \frac{1}{2m_2}(I_1 - I_2)^2 + v_0 I_1 = 0. \tag{15}$$

Centered at $\left(\frac{-v_0 \cos\theta}{\frac{\cos^2\theta}{m_1} + \frac{1-\sin(2\theta)}{m_2}}, \frac{v_0 \sin\theta}{\frac{\sin^2\theta}{m_1} + \frac{1+\sin(2\theta)}{m_2}} \right)$, the ellipse rotates from the x-axis by an angle $\theta = \frac{1}{2}\arctan\left(-\frac{2m_1}{m_2}\right)$, as shown in Fig. 3. It is tangent to the I_2-axis and the line $I_1 = -2m_1 v_0$ at the origin and the point $(-2m_1 v_0, -2m_1 v_0)$, respectively.[3]

The impulse curve is monotone in the sense that I_1 and I_2 never decrease. This is clear if the state is S_2 or S_3 in which one of the impulses increases while the other does not vary.
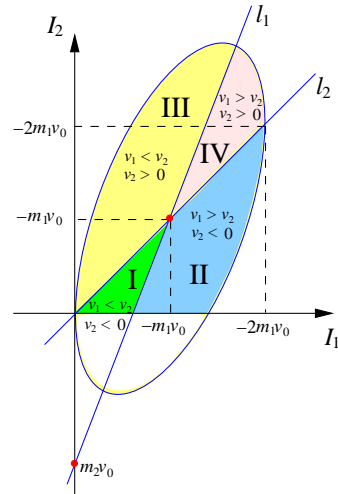
Fig. 3. Impulse plane.

---

[3] The two horizontal bounding lines are $I_2 = (-m_1 \pm \sqrt{m_1 m_2})v_0$ with points of tangency to the ellipse at $I_1 = -m_1 v_0$.

(a)

state	v_1	v_2	I_1	I_2	Comp. Res.
S_1	0.6088	0.3573	3.6085	3.9661	C2-C1-R2
S_3	0.9661	0	3.9661	3.9661	
S_1	2.4414	−0.1211	5.4414	5.3202	R1
S_2	2.4414	0.7355	5.4414	6.1769	C2-R2

(b)

(c)
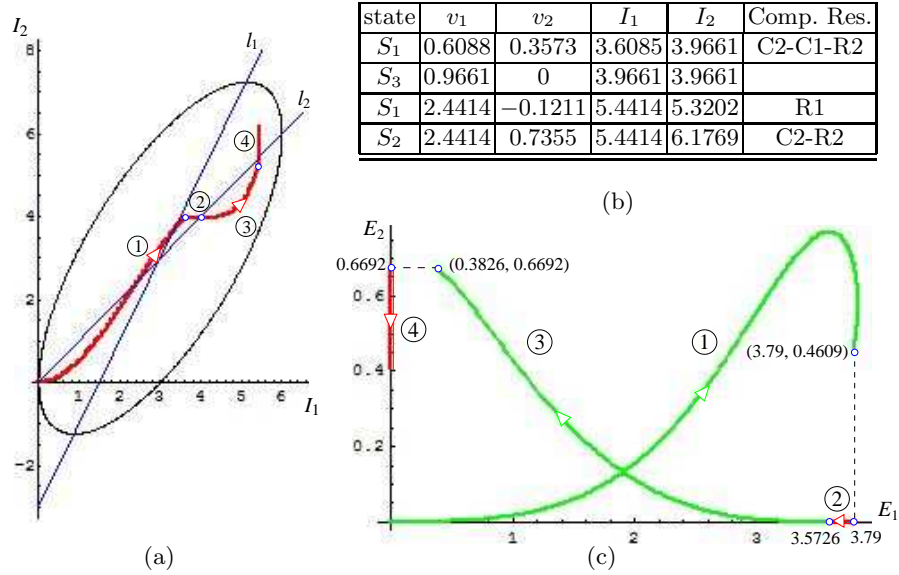
Fig. 4. The impulse and energy curves for a collision of two balls as in Fig. 1 with masses $m_1 = m_2 = 1$kg, the stiffness ratio $\frac{k_2}{k_1} = 10$, the coefficients of restitution $e_1 = \sqrt{0.9}$ and $e_2 = \sqrt{0.4}$, and the upper ball velocity $v_0 = -3$m/s.

After S_1 starts, the strain energies $E_1, E_2 > 0$, which implies the derivative $dI_2/dI_1 = \sqrt{k_2 E_2}/\sqrt{k_1 E_1} > 0$, hence the monotonicity.

Add two lines ℓ_1 and ℓ_2 defined by equations (12). Referred to as the *compression lines*, they partition the feasible elliptic region ($I_1 \geq 0$) into four smaller regions I–IV. The impulse curve evolves from the origin into region I within the state S_1 as $\frac{dI_2}{dI_1}$ increases from 0. As I_1 increases unconstrained, the curve will cross ℓ_1 (or ℓ_2) when the ball-ball impact (or the ball-table impact) ends compression. During the state S_2, the curve stays to the right of the line ℓ_1, and evolves vertically upward, ending either inside region IV (in which case the collision ends) or on the line ℓ_1 for a transition to S_1. Similarly, during S_3, the curves stays to the left of ℓ_2 and evolves horizontally to the right, ending either inside the region IV or on the line ℓ_2 for a transition to S_1.

Fig. 4 illustrates a collision instance which results in a sequence of four states S_1, S_3, S_1, S_2. In (a), the impulse curve is plotted, along with the bounding ellipse: $-3I_1 + \frac{1}{2}I_1^2 + \frac{1}{2}(I_1 - I_2)^2 = 0$ and the two compression lines $\ell_1: -3 + 2I_1 - I_2 = 0$ and $\ell_2 : I_1 = I_2$. The impulse segments corresponding to different states are labeled in the order and separated by the dots. The first segment (of a S_1 state) crosses ℓ_2 before ℓ_1, indicating that the ball-table impact goes into restitution before the ball-ball impact. The ball-table impact subsequently finishes restitution. This is marked as C2-C1-R2 in table (b), where each row describes the status at the end of a state. Diagram (c) in the

figure plots the evolution of the elastic energies E_1 and E_2 with four segments also labeled in the state order. It shows energy losses at the end of all but the second states. The loss in the total (elastic and dynamic) energy E during the collision is calculated to be 1.2494.

Suppose restitution were decided by impulse accumulation according to Poisson's hypothesis for single impact. The same collision would generate an impulse curve exiting the bounding ellipse (15) in the fourth state — the increase of I_1 to the required value 5.906 would result in a negative elastic energy ($E_1 = -1.01$).

Every state terminates. This is trivial for S_2 and S_3 for which ΔI_1 and ΔI_2 are given in Section 2.2. Within the state S_1, the 'primary impulse' must stop increasing because the impulse curve is bounded inside the ellipse (15).

Denote by $I_1^{(i)}$ and $I_2^{(i)}$ the values of the two impulses at the end of the ith state. The sequence $\{(I_1^{(i)}, I_2^{(i)})\}$ is monotone non-decreasing. In case it is finite, the state transitions terminate with $v_1 \geq v_2 \geq 0$ according to the diagram in Fig. 2 as the impulse curve stops inside region IV in Fig. 3 or on it boundary.[4] In case the sequence is infinite, because it is bounded inside the ellipse (15), by a result from calculus it must converge to some point (I_1^*, I_2^*). We can show that this point must lie on the boundary of region IV.

Theorem 3. *The state transitions will either terminate with $v_1 \geq v_2 \geq 0$ or the generated impulse sequence will converge with either $v_1 = v_2 \geq 0$ or $v_1 > v_2 = 0$.*

As v_0 scales by a factor of s, we can show that throughout the collision the impulses I_1, I_2 and the velocities v_1, v_2 scale by s while the elastic energies E_1 and E_2 scale by s^2. The differential equation (10) still holds after the scaling, as well as the conditions (12) for ending of compressions and the conditions on state transitions.

Theorem 4. *At the end of the collision, the ratios v_1/v_0 and v_2/v_0 are constants depending on m_1, m_2, e_1, e_2 and the stiffness ratio k_1/k_2 only.*

2.4 Preliminary Experiment

To validate the collision model, we let a ping pong ball $\mathcal{B}_1$ fall onto another one $\mathcal{B}_2$ resting on a plexiglass block. The ball has mass 0.00023kg and radius 0.019m. The block is placed horizontally on the marker tray of a (vertical) office whiteboard, and against a vertical axis ℓ drawn on the board. The ball $\mathcal{B}_1$ is held in the hand. Both balls are positioned almost in contact with the whiteboard such that ℓ "passes through" their centers in the frontal view.

To measure the coefficient of restitution e_2 between a ball and the plexiglass surface, we drop the ball from certain height h_1 onto the surface and record the rebounding height h_2 (on the axis by human vision). Thus

---

[4] The curve will reach the bounding ellipse at termination only if $e_1 = e_2 = 1$.

$e_2 \approx \sqrt{h_2/h_1}$. Sixteen measurements from different heights (with four balls) have generated a mean estimate of 0.846529 with a standard deviation of 0.020827. To measure the coefficient of ball-ball restitution e_1, $\mathcal{B}_2$ is held steady on the surface, and $\mathcal{B}_1$ is dropped from the same height onto $\mathcal{B}_2$ multiple times with the highest rebound (from the closest-to-a-perfect hit) recorded. The mean value of e_1 calculated over eight different dropping heights is 0.807755 with standard deviation 0.021231.

A collision trial involves dropping $\mathcal{B}_1$ from a fixed height onto $\mathcal{B}_2$ multiple times, and choosing the one with the highest rebounds of both balls. The input velocity v_0 and the output velocities v_1 and v_2 are calculated. Results from ten trials, each with a different dropping height, are plotted in Fig. 5 as pairs of points $(-v_0, v_1)$ and $(-v_0, v_2)$. Also shown are the two lines v_1 and v_2 as v_0 varies from -2m/s to -4m/s. Despite the rather primitive setup and measurement method, the re-

Fig. 5. Collisions between two ping pong balls and a plexiglass surface: experimental results (dots) vs. predictions (lines) by the impact model (with guess $k_2/k_1 = 10$).

sult suggests a reasonably good match between the model and the physical collision process.

3   Shooting a Billiard

We apply the impact model to the problem of a cue stick shooting the cue ball in the game of pool, as illustrated in Fig. 6. The cue stick has initial velocity $\boldsymbol{v}_{c0}$. Let $\boldsymbol{c}$ be the unit vector $\boldsymbol{v}_{c0}/\|\boldsymbol{v}_{c0}\|$, $\boldsymbol{n}$ the unit normal at the point of impact on the ball, and $\boldsymbol{z}$ the unit normal at the table contact. The condition $\boldsymbol{n} \cdot \boldsymbol{c} < 0$ must hold for the shot to happen. During the shot, we assume that the cue stick is constrained to move along $\boldsymbol{c}$ or $-\boldsymbol{c}$.[5] The cue stick has velocity $\boldsymbol{v}_c$, the ball has velocity $\boldsymbol{v}$ and angular velocity $\boldsymbol{\omega}$, all varying during the shot.

Fig. 6. Pool shot.

Denote by $\boldsymbol{I}_1$ and $\boldsymbol{I}_2$ the impulses at the cue-ball and the ball-ball contacts, respectively, as shown in the figure. The impulse $\boldsymbol{I}_1$ consists of a normal component $I_{1n}\boldsymbol{n}$ and a tangential component $\boldsymbol{I}_{1\perp}$. The impulse $\boldsymbol{I}_2$ consists of a vertical component $I_{2z}\boldsymbol{z}$ and a horizontal component $\boldsymbol{I}_{2\perp}$. We have $I_{1n} > 0$ or $I_{2z} > 0$ whenever the corresponding impact is active.

---
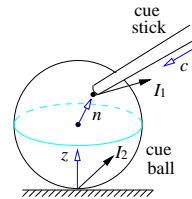
[5] This is the case with our design of a mechanical cue stick to be shown in Fig. 8.

Two virtual springs, with stiffnesses k_{cb} and k_{bt}, are attached at the points of impact in alignment with the normals $\boldsymbol{n}$ and $\boldsymbol{z}$, respectively. Based on the impact model, the shot by the cue stick has three states: S_1 (illustrated in Fig. 7) during which both the ball-ball and the ball-table impacts are active, S_2 during which only the ball-table impact is active, and S_3 during which only the ball-ball impact is active. The shot starts with S_1 and ends in either S_2 or S_3.
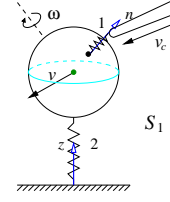
Fig. 7. State S_1.

Denote by $\boldsymbol{v}_{cb}$ the relative velocity of the cue stick to the ball, and by $\boldsymbol{v}_{bt}$ that of the ball to the pool table. The state transition diagram has the same structure as that in Fig. 2 except in the transition conditions, $v_1 - v_2$ and v_2 are respectively replaced by the normal velocity components $\boldsymbol{v}_{cb} \cdot \boldsymbol{n}$ and $\boldsymbol{v}_{bt} \cdot \boldsymbol{z}$. A cue-ball impact is in compression when $\boldsymbol{v}_{cb} \cdot \boldsymbol{n} < 0$. A ball-table impact is in compression when $\boldsymbol{v}_{bt} \cdot \boldsymbol{z} < 0$.

If the cue stick shoots the ball below its equator (i.e., $\boldsymbol{n} \cdot \boldsymbol{z} < 0$) or at the equator horizontally or upward, only the cue-ball impact exists. In this case, the transition diagram has only one state — S_3.

3.1   Dynamics and Impact State Analysis

The symbols (0) and Δ carry the same meanings as in Section 2. For instance, $\Delta \boldsymbol{v}_{cb} = \boldsymbol{v}_{cb} - \boldsymbol{v}_{cb}^{(0)}$ is the change in the relative velocity of the cue stick to the cue ball during a state from its starting value $\boldsymbol{v}_{cb}^{(0)}$.

Let M be the mass of the cue stick. Let the ball have radius r and mass m, thus angular inertia $\frac{2}{5}mr^2$. Changes in the velocities during a state can be expressed in terms of the impulse accumulations $\Delta \boldsymbol{I}_1$ and $\Delta \boldsymbol{I}_2$:

$$\Delta \boldsymbol{v}_c = \frac{1}{M}(\Delta \boldsymbol{I}_1 \cdot \boldsymbol{c})\boldsymbol{c}, \qquad\qquad \Delta \boldsymbol{v} = \frac{1}{m}(\Delta \boldsymbol{I}_2 - \Delta \boldsymbol{I}_1), \quad (16)$$

$$\Delta \boldsymbol{\omega} = \frac{5}{2}\frac{1}{mr^2}\Big(r\boldsymbol{n} \times (-\Delta \boldsymbol{I}_1) + (-r\boldsymbol{z}) \times \Delta \boldsymbol{I}_2\Big), \qquad\qquad (17)$$

$$\Delta \boldsymbol{v}_{cb} = \Delta \boldsymbol{v}_c - \Delta \boldsymbol{v} - \Delta \boldsymbol{\omega} \times (r\boldsymbol{n}), \qquad \Delta \boldsymbol{v}_{bt} = \Delta \boldsymbol{v} - \Delta \boldsymbol{\omega} \times (r\boldsymbol{z}). \quad (18)$$

To find out how the normal impulses $I_{1n} = \boldsymbol{I}_1 \cdot \boldsymbol{n}$ and $I_{2z} = \boldsymbol{I}_2 \cdot \boldsymbol{z}$ are related to each other in the state S_1, we notice that the two virtual springs at the cue-ball and the ball-table contacts have their lengths change at the rates $\dot{x}_1 = \boldsymbol{n} \cdot (\boldsymbol{v}_{cb}^{(0)} + \Delta \boldsymbol{v}_{cb})$ and $\dot{x}_2 = \boldsymbol{z} \cdot (\boldsymbol{v}_{bt}^{(0)} + \Delta \boldsymbol{v}_{bt})$, respectively. From these rates, $\dot{I}_{1n} = -k_{cb}x_1$, and $\dot{I}_{2z} = -k_{bt}x_2$, we obtain the derivatives $\frac{dx_1}{dI_{1n}}$ and $\frac{dx_2}{dI_{2z}}$ as linear expressions in $\Delta \boldsymbol{I}_1$ and $\Delta \boldsymbol{I}_2$ over $-k_{cb}x_1$ and $-k_{bt}x_2$, respectively. Multiplying away the denominators in the derivative equations and integrating both sides of each equation, we obtain the changes in the elastic energies:

$$\Delta E_1 = E_1 - E_1^{(0)} = -\boldsymbol{n} \cdot \left(\Delta I_{1n}\boldsymbol{v}_{cb}^{(0)} + \Big(\frac{1}{M}\boldsymbol{cc}^T + \frac{1}{m}\Big)D_1 - \frac{1}{m}D_2 \right), (19)$$

$$\Delta E_2 = E_2 - E_2^{(0)} = -\boldsymbol{z} \cdot \left(\Delta I_{2z} \boldsymbol{v}_{\text{bt}}^{(0)} - \frac{1}{m} D_3 \right) - \frac{1}{m} D_4, \tag{20}$$

where the integrals during the state are defined as $D_1 = \int_{I_{1n}^{(0)}}^{I_{1n}} \Delta \boldsymbol{I}_1 \, dI_{1n}$, $D_2 = \int_{I_{1n}^{(0)}}^{I_{1n}} \Delta \boldsymbol{I}_2 \, dI_{1n}$, $D_3 = \int_{I_{2z}^{(0)}}^{I_{2z}} \Delta \boldsymbol{I}_1 \, dI_{2z}$, and $D_4 = \frac{1}{2} \Delta I_{2z}^2$. This sets up a differential relationship between I_{1n} and I_{2z}:

$$\frac{dI_{2z}}{dI_{1n}} = \frac{\dot{I}_{2z}}{\dot{I}_{1n}} = \frac{-k_{\text{bt}} x_2}{-k_{\text{cb}} x_1} = \sqrt{\frac{k_{\text{bt}}}{k_{\text{cb}}}} \cdot \sqrt{\frac{E_2^{(0)} + \Delta E_2}{E_1^{(0)} + \Delta E_1}}. \tag{21}$$

The system of equations (19)–(21), along with a contact mode analysis, determines the evolution within the state S_1. A closed-form solution does not exist in general. Numerical integration is performed as follows.

Entering a state, we need to set dI_{1n} to h and compute dI_{2z}/dI_{1n} if at the start of the shot or the previous state is S_3, or set dI_{2z} to h and compute dI_{1n}/dI_{2z} if the previous state is S_2. The tangential impulse increments $d\boldsymbol{I}_{1\perp}$ and $d\boldsymbol{I}_{2\perp}$, as well as D_1, D_2, D_3, D_4, are also initialized. This is similar to that for the two-ball collision as described right before Section 2.1 but is much more involved since we need also determine the contact modes.

After initialization, iterate until one of the impacts ends restitution. At each iteration step, update $\boldsymbol{v}_{\text{cb}}, \boldsymbol{v}_{\text{bt}}$ according to (18), and E_1, E_2 according to (19)–(20). In case one impact is starting restitution, set maximum elastic energy $E_{1\max}$ or $E_{2\max}$ accordingly. Compute dI_{1n} and dI_{2z} by (21), and $\boldsymbol{I}_{1\perp}$ and $\boldsymbol{I}_{2\perp}$ based on a contact mode analysis to be described below. The iteration step finishes with updating the values of $\Delta \boldsymbol{I}_1, \Delta \boldsymbol{I}_2, D_1, D_2, D_3, D_4$.

Contact Modes   Contact modes depend on the tangential components $\boldsymbol{v}_{\text{cb}\perp}$ and $\boldsymbol{v}_{\text{bt}\perp}$ of the two contact velocities $\boldsymbol{v}_{\text{cb}}$ and $\boldsymbol{v}_{\text{bt}}$. Let μ_{cb} and μ_{bt} be the coefficients of friction between the cue tip and the ball and between the ball and the table, respectively. When a tangential velocity, say, $\boldsymbol{v}_{\text{cb}\perp}$, is not zero, the cue tip is sliding on the ball. We have $d\boldsymbol{I}_{1\perp} = -\mu_{\text{cb}} dI_{1n} \cdot \hat{\boldsymbol{v}}_{\text{cb}\perp}$ under Coulomb's law, where $\hat{\boldsymbol{v}}_{\text{cb}\perp} = \boldsymbol{v}_{\text{cb}\perp}/\|\boldsymbol{v}_{\text{cb}\perp}\|$. Similarly, $d\boldsymbol{I}_{2\perp} = -\mu_{\text{bt}} dI_{2z} \cdot \hat{\boldsymbol{v}}_{\text{bt}\perp}$ when the ball is sliding on the table.

When one tangential velocity is zero, there are three cases: (1) $\boldsymbol{v}_{\text{cb}\perp} = 0$ but $\boldsymbol{v}_{\text{bt}\perp} \neq 0$, (2) $\boldsymbol{v}_{\text{bt}\perp} = 0$ but $\boldsymbol{v}_{\text{cb}\perp} \neq 0$, and (3) $\boldsymbol{v}_{\text{cb}\perp} = 0$ and $\boldsymbol{v}_{\text{bt}\perp} = 0$. We here treat the first case only as the other two cases can be handled similarly.

In case (1), $d\boldsymbol{I}_{2\perp} = -\mu_{\text{bt}} dI_{2z} \cdot \hat{\boldsymbol{v}}_{\text{bt}\perp}$. We obtain the derivative of $\boldsymbol{v}_{\text{cb}\perp}$ with respect to I_{1n} in terms of those of the tangential impulses $\boldsymbol{I}_{1\perp}$ and $\boldsymbol{I}_{2\perp}$. To stay in sticking contact, $d\boldsymbol{v}_{\text{cb}\perp}/dI_{1n} = 0$, which determines the value of $d\boldsymbol{I}_{1\perp}/dI_{1n}$. If $\|d\boldsymbol{I}_{1\perp}/dI_{1n}\| \leq \mu_{\text{cb}}$, the contact stays sticking. Otherwise, the contact starts sliding in the direction of $d\boldsymbol{v}_{\text{cb}\perp}/dI_{1n}$, which can be solved.

Ball-Table Impact Only   In the state S_2, $E_1 = 0$ and $\boldsymbol{I}_1 = 0$. In the case that S_2 begins during compression, we set the maximum elastic energy $E_{2\max} = E_2^{(0)} + \frac{1}{2} m (\boldsymbol{v}_{\text{bt}}^{(0)} \cdot \boldsymbol{z})^2$. From (16)–(18) under $\Delta \boldsymbol{I}_1 = 0$, the change

in the tangential velocity is $\Delta \boldsymbol{v}_{\text{bt}\perp} = (1 - \boldsymbol{z}\boldsymbol{z}^T)\Delta \boldsymbol{v}_{\text{bt}} = \frac{7}{2m}\Delta \boldsymbol{I}_{2\perp}$. So $\boldsymbol{v}_{\text{bt}\perp}$ and $\boldsymbol{I}_{2\perp}$ will not change their directions during the state. Once $\boldsymbol{v}_{\text{bt}\perp}$ reduces to zero, it will stay zero so as not to contradict Coulomb's law. To make $\boldsymbol{v}_{\text{bt}}^{(0)}$ zero, $\Delta \boldsymbol{I}_{2\perp} = -m\boldsymbol{v}_{\text{bt}}^{(0)}$, which requires $\Delta I_{2z} \geq m\frac{\|\boldsymbol{v}_{\text{bt}}^{(0)}\|}{\mu_{\text{bt}}}$. Also, S_2 would switch to the state S_1 when $\boldsymbol{v}_{\text{cb}} \cdot \boldsymbol{n} = 0$. We hypothesize the outcome of S_2 (a transition to S_1 or the end of collision), and in the first case, the contact mode (sticking or sliding). Then we test these hypotheses by checking some derived inequalities which depend on $\boldsymbol{v}$, $\boldsymbol{v}_{\text{c}}^{(0)}$, $\boldsymbol{v}_{\text{bt}}^{(0)}$, $E_2^{(0)}$, ΔE_2, and $E_{2\max}$.

Cue-Ball Impact Only   Entering the state S_3 from S_1, the ball-table impact had just finished restitution, so $\boldsymbol{v}_{\text{bt}}^{(0)} \cdot \boldsymbol{z} > 0$. Substituting $\Delta \boldsymbol{I}_2 = 0$ into (18), we obtain the change in the tangential velocity: $\Delta \boldsymbol{v}_{\text{cb}\perp} = \frac{1}{M}(\boldsymbol{c} \cdot \Delta \boldsymbol{I}_1)\boldsymbol{c}_\perp + \frac{7}{2m}\Delta \boldsymbol{I}_{1\perp}$. Two special cases, $\boldsymbol{c} = \boldsymbol{n}$ and $\boldsymbol{c} \cdot \boldsymbol{z} = \boldsymbol{n} \cdot \boldsymbol{z} = 0$, can be treated with analyses similar to that for the case of ball-table impact only.

Generally, $\boldsymbol{I}_{1\perp}$ varies its direction along a curve in the tangent plane. Numerical integration similar to that described earlier for the two-impact state is employed. The procedure is nevertheless simpler given only one impulse $\boldsymbol{I}_1$.

3.2   Billiard Simulation

Table 1 shows four different shots and the trajectories[6] resulting from three of them. With some simplifications[7], the ball trajectory is completely determined by the x and y components of its velocity $\boldsymbol{v}$ and angular velocity $\boldsymbol{\omega}$. It is known that the ball will first slide along a parabolic arc (unless $\boldsymbol{\omega} \cdot \boldsymbol{v} = 0$) and then roll along a straight line before coming to a stop.

The first shot, vertical but not through the ball center, yields a straight trajectory in figure (a). The second shot (figure (b)), horizontal along the x-axis, hits the point at the polar angle $\frac{3\pi}{4}$ on the ball's equator. Due to friction, the ball trajectory forms a smaller angle with the x-axis than with the y-axis, exhibiting some effect of English. The third is a jump shot in the x-z plane. The last one, shown in figure (c), is a massé shot with the cue erected.

4   Discussion and Future Work

The introduced impact model makes use of the fact that the velocity and angular velocity of a body in simultaneous collisions are linear in the impulses at its contact points (with other bodies) like in (5)–(6) or (16)–(17). The linearity carries over to an object of arbitrary shape with angular inertia matrix Q. Suppose the forces $\boldsymbol{f}_i$ are applied on the object at the locations $\boldsymbol{r}_i$.

---

[6] The trajectory equations are omitted, though some can be found in [11].

[7] We ignore the effects on the trajectory due to (possibly) multiple collisions between the ball and the table.

shot	n	$v_{\mathrm{c}}^{(0)}$	v	ω
vertical	$\frac{(-1,-2,1)}{\sqrt{6}}$	$(0,0,-2)$	$(0.3963, 0.7926, 0.4506)$	$(27.97, -13.98, 0)$
horizontal	$(-\frac{\sqrt{2}}{2}, -\frac{\sqrt{2}}{2}, 0)$	$(0.8, 0, 0)$	$(0.6299, 0.4614, 0)$	$(0, 0, 10.42)$
jump	$(-\frac{\sqrt{2}}{2}, 0, -\frac{\sqrt{2}}{2})$	$(1, 0, -1)$	$(1.169, 0, 0.1883)$	$(0, 13.15, 0)$
massé	$\frac{(-2,-1,12)}{\sqrt{149}}$	$(4, 0, -16)$	$(-0.3253, 0.2938, 6.232)$	$(-88.48, 179.8, -3.178)$

(a)   (b)   (c)
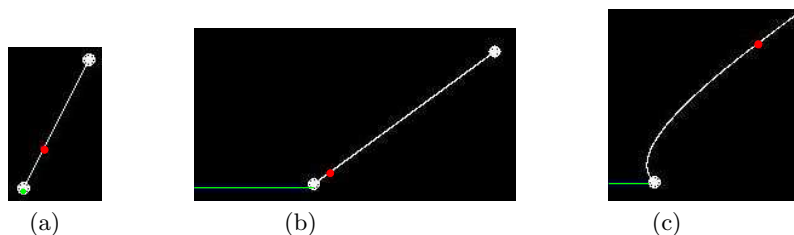
Table 1. Four shots at the cue ball (with the x-y plane on the pool table). Trajectories (a), (b), (c) are produced by the 1st, 2nd, 4th shots, respectively. On each trajectory, the red dot marks where sliding switches to pure rolling; and the green line represents the cue stick. We use the following measured physical constants: $m = 0.1673$kg, $M = 0.5018$kg, $r = 0.0286$m, $\mu_{\mathrm{bt}} = 0.152479$, $e_{\mathrm{cb}} = 0.656532$, and $e_{\mathrm{bt}} = 0.51625$. We set $\mu_{\mathrm{cb}} = 0.4$ [14] and the stiffness ratio $k_{\mathrm{cb}}/k_{\mathrm{bt}} = 1.5$.

Integrating the dynamic equation $\sum_i \boldsymbol{r}_i \times \boldsymbol{f}_i = Q\dot{\boldsymbol{\omega}} + \boldsymbol{\omega} \times Q\boldsymbol{\omega}$ over the duration Δt of an impact, we obtain $\sum_i \boldsymbol{r}_i \times \boldsymbol{I}_i = Q\Delta\boldsymbol{\omega}$ since $\boldsymbol{\omega}$ is bounded.

The state transition diagram can deal with three or more impact points via state partitioning based on which impacts are instantaneously "active" and which are not. A transition happens whenever the set of active impacts changes. The evolution within a state is driven by the primary impulse. The elastic energy at a contact can still be expressed in terms of the impulses affecting the two involved bodies as in (8)–(9). A differential relationship like (21) holds between the active normal impulses at two contact points.

We would like to compare the model with other existing models [3,8,5] on multiple impacts. Our main effort, though, will be experimental verification of the impact model for billiard shots. A shooting mechanism has been designed as shown in Fig. 8. It includes a steel cue stick constrained to linear motions by ball bearings inside an aluminum box. The cue stick can be elevated by adjusting the slope of the attached incline. We plan to examine issues like area contact, shearing effect of the cue tip, bending of the cue stick, gravity, etc.

Fig. 8. A mechanical cue stick.

The long term objective is to design a robot able to play billiards with human-level skills based on understanding of the mechanics. To our knowledge, none of the developed systems [13,10,7] perform shots based on the mechanics of billiards, or have exhibited real shooting skills.

References

1. S. Ahmed, H. M. Lankarani, and M. F. O. S. Pereira. Frictional impact analysis in open-loop multibody mechanical systems. *J. Applied Mechanics*, 121:119–126, 1999.
2. M. Anitescu and F. A. Porta. Formulating dynamic multi-rigid-body contact problems with friction as solvable linear complementarity problems. *ASME J. Nonlinear Dynamics*, 14:231–247, 1997.
3. D. Baraff. Analytical methods for dynamic simulation of non-penetrating rigid bodies. *Computer Graphics*, 23(2):223-232, 1989.
4. R. M. Brach. Rigid body collisions. *J. Applied Mechanics*, 56:133–137, 1989.
5. A. Chatterjee and A. Ruina. A new algebraic rigid-body collision law based on impulse space considerations. *J. Applied Mechanics*, 65:939–951, 1998.
6. I. Han and B. J. Gilmore. Impact analysis for multiple-body systems with friction and sliding contact. In D. P. Sathyadev (ed.), *Flexible Assembly Systems*, 1989.
7. K. H. L. Ho, T. Martin, and J. Baldwin. Snooker robot player — 20 years on. In *Proc. IEEE Symp. Comp. Intell. Games*, pp. 1–8, 2007.
8. A. P. Ivanov. On multiple impact. *J. Applied Math. Mechanics*, 59(6):887-902, 1995.
9. J. B. Keller. Impact with friction. *J. Applied Mechanics*, 53(1):1–4, 1986.
10. F. Long *et al.* Robotic pool: an experiment in automatic potting. In *Proc. IEEE/RSJ Int. Conf. Intell. Robots Syst.*, pp. 2520–2525, 2004.
11. W. C. Marlow. *The Physics of Pocket Billiards*. Marlow Advanced Systems Technologies, 1994.
12. M. T. Mason. *Mechanics of Robotic Manipulation*. The MIT Press, 2001.
13. A. W. Moore, D. J. Hill, and M. P. Johnson. An empirical investigation of brute force to choose features, smoothers and function approximators. In S. J. Hanson *et al.*, ed., *Computational Learning Theory and Natural Learning*, pp. 361–379. The MIT Press, 1995.
14. `http://physics.usyd.edu.au/~cross/Billiards.htm`.
15. E. J. Routh. *Dynamics of a System of Rigid Bodies*. MacMillan and Co., 1913.
16. D. E. Stewart and J. C. Trinkle. An implicit time-stepping scheme for rigid body dynamics with inelastic collisions and Coulomb friction. *Int. J. Numer. Methods Engr.*, 39:2673–2691, 1996.
17. D. E. Stewart. Rigid-body dynamics with friction and impact. *SIAM Review*, 42(1):3–39, 2000.
18. Y. Wang and M. T. Mason. Two-dimensional rigid-body collisions with friction. *J. Applied Mechanics*, 59(635-642), 1991.